Title: Effects of Crystal Habit on the Sticking Propensity of Ibuprofen—A Case Study

Authors: D. Hooper, F.C. Clarke, R. Docherty, J.C Mitchell, M.J. Snowden

PII: S0378-5173(17)30809-8
DOI: http://dx.doi.org/10.1016/j.ijpharm.2017.08.091
Reference: IJP 16944

To appear in: *International Journal of Pharmaceutics*

Received date: 17-5-2017
Revised date: 17-8-2017
Accepted date: 19-8-2017

Please cite this article as: Hooper, D., Clarke, F.C., Docherty, R., Mitchell, J.C, Snowden, M.J., Effects of Crystal Habit on the Sticking Propensity of Ibuprofen—A Case Study.International Journal of Pharmaceutics http://dx.doi.org/10.1016/j.ijpharm.2017.08.091

Effects of Crystal Habit on the Sticking Propensity of Ibuprofen - A Case Study

D. Hooper[a,b*], F.C. Clarke[b], R. Docherty[b], J.C Mitchell[a*‡], M.J. Snowden[a]

[a]Faculty of Engineering and Science, University of Greenwich, Medway, ME4 4TB, UK.

[b]Pfizer Ltd., Ramsgate Road, Sandwich, CT13 9NJ, UK.

[‡] Corresponding Author;
Email: J.Mitchell@Greenwich.ac.uk
Phone: +44 (0)1634 883358
Fax: +44 (0)1634 883044

Graphical Abstract

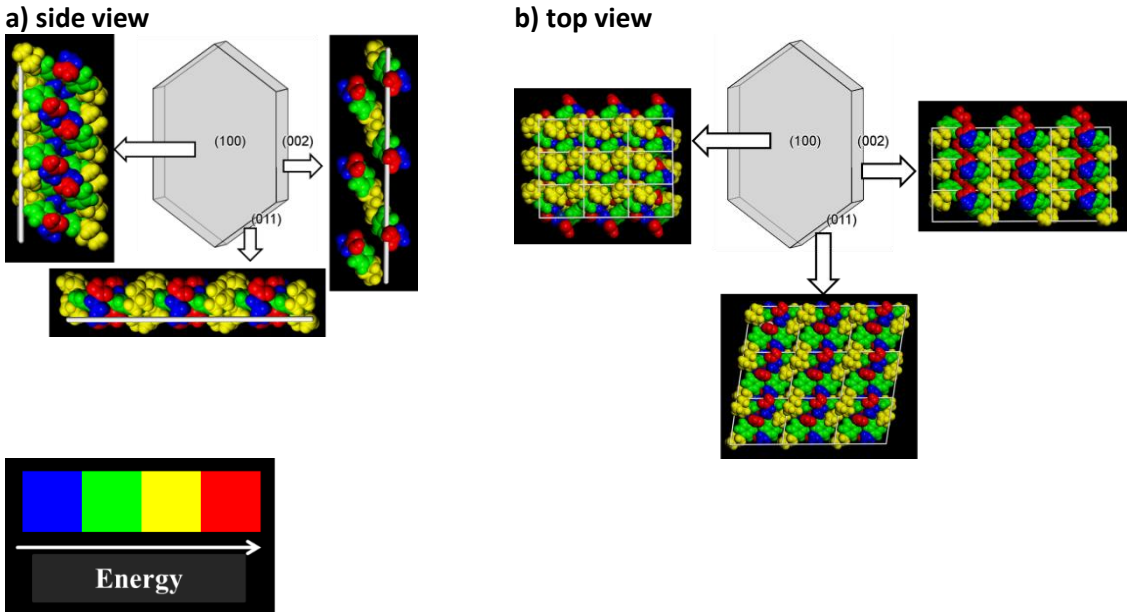

Abstract

This study demonstrates the effect of active pharmaceutical ingredient (API) particle habit on the sticking propensity of ibuprofen. Four diverse crystal habits with similar physico chemical properties are reported and the sticking propensity was found to increase with shape regularity. The surface energy of the extreme habits were shown to be different where particles that were more regular in shape exhibited surface energies of 9 mJ/m^2 higher than those that were needle-like in habit. Computational and experimental data reveals that the increase in surface energy of the regular shaped particles can be attributed to the increase in the specific (polar) component, which is due to greater presence of faces which contain the carboxylic acid functionality at the surface. The increase in the specific energy component is shown to correlate with the sticking propensity of ibuprofen. It is

proposed that investigation of the chemical causality of sticking, for this API and others, using the techniques demonstrated in this paper will be of increasing importance.

Keywords: particle shape; surface energy; punch sticking; crystal chemistry

1 Introduction

During API development, critical quality attributes (CQAs) are set out in the final specifications for the drug product [1]. Solid form and particle size distributions are CQAs with particle shape and surface energy often neglected due to the lack of understanding of their impact.

The engineering of particles with desired properties has become increasingly important and this has led to pharmaceutical Materials Science emerging as a foundation of Quality by Design (QbD) with solid form, crystallization and particle engineering being core elements linking the drug product functional form to the final steps of the API manufacturing process [2, 3]. More recently the importance of the Materials Science tetrahedron, depicting the relationships between internal structure, particle properties, material processing and performance of a drug product, has been described [4].

For a given API the crystal habit is typically specified through the crystallisation protocol. Different crystal faces of the API produced exhibit different surface chemistry and hence interact differently with solvents, process impurities and excipients. These different crystal faces can be present in different proportions for a given API. The changes in crystal habit, which are generally not controlled in specifications, in combination with particle size can lead to different chemical and physical stabilities, biopharmaceutical properties and processing behaviour (API and drug product) [5, 6].

This work seeks to outline some of the recent progress on the application of emerging computer modelling technologies for the design strategy of advanced functional particulate products [7]. The paper highlights the opportunity for bridging across the chemical, analytical and manufacturing disciplines with a particular focus on understanding punch sticking.

One of the major issues affecting the production of pharmaceutical tablets is the formulation adhering to the tooling surfaces, known as punch sticking. Punch sticking compromises the manufacturing process. Many attempts in the literature have been made to determine the elusive root cause of this phenomenon however no single root cause has been identified [7, 8]. It is known that sticking may be due to API adherence even when it is present in a formulation at low concentrations [9] and many complex processing and environmental mechanisms such as speed/force/dwell time [10], temperature/humidity [11], punch geometry/quality where quality is defined as surface roughness and if the punch contains any defects[10] and lubrication [12] have been shown to contribute.

There is still a lack of understanding between the particle habit and surface energy of an API and their role in punch sticking despite some recent efforts [7, 13]. One of the challenges often faced when trying to link these properties is punch sticking is not detected until full scale manufacture and there is a technology gap relating to a small scale test to predict sticking especially when APIs are limited in quantity. This work presents a simple science of scale tool to quantify the sticking of an API with different particle habits and similar physico-chemical properties in combination with emerging computational tools to explore the crystal chemistry in relation to surface energies.

2 Materials and Methods

2.1 Computational Tools

This study focuses on racemic ibuprofen *(RS)*-ibuprofen. The Cambridge Structural Database (CSD) was interrogated for *(RS)*-ibuprofen structures using ConQuest (CCDC 1.18, 2016). The criteria for this search were *R*-factor of less than 0.0075 and no metals allowed. The crystal structure selected for ibuprofen was IBPRAC and the carboxylic acid hydrogen bonding distance for this hit was measured and compared to all other hits with this functionality using the search criteria above.

The .cif for IBPRAC, was imported into Materials Studio (v7.0, 2013) and the intermolecular interactions were calculated using the following force fields: geometry optimised/fractional charges assigned using COMPASS II/Tripos 5.2 force field, respectively [14, 15]. All further calculations were performed using these parameters. HABIT98 [16, 17] was used to calculate the strength of the non-bonded intermolecular interactions (intrinsic synthons) and lattice energy (E_{cr}). In order to determine if the force field assigned accurately estimated the intermolecular strength of interactions the lattice energy was compared to the sublimation enthalpy (ΔH_{sub}) as the relationship shown below exists:

$$E_{cr} = \Delta H_{sub} - 2RT \quad (1)$$

Where R is the gas constant and T is temperature.

To further validate the force field, the strength of the most dominant intermolecular interaction was compared to validation work published by Dunitz and Gavezzotti [18].

The Bravais, Friedel, Donnay and Harker (BFDH) [19-21] method was used to predict the most likely growth surfaces based on the rule which states the faces with the largest interplanar spacing (d_{hkl}) are likely to be the most morphologically important at the surface [22, 23]. The lattice energy (E_{cr}) per surface was split into slice energy (E_{sl}) and attachment energy (E_{att}) based on the equation shown below [22] :

$$E_{cr} = E_{sl} + E_{att} \quad (2)$$

The morphology of ibuprofen was predicted using the attachment energy model which states that the faces with the lowest attachment energies will be the slowest growing and therefore be the most morphologically important [24].

Previously published studies have revealed that during crystallisation of ibuprofen only three of the surfaces predicted by the BFDH and attachment energy models are present [25-27]. These faces are {1 0 0}, {0 1 1} and {0 0 2} and Materials Studio was used to visualise the chemistry present at each surface (extrinsic synthons).

The relative attachment energy of each face was expressed as centre to face distances then Mercury (CCDC 3.9, 2016) was used to visualise the external morphology. The surface energy of these faces was calculated using the attachment energy calculation shown below [24]:

$$\gamma_{hkl} = \frac{ZE_{att}d_{hkl}}{2V_{cell}N_A} \quad (3)$$

Where Z is the numbers of molecules in the unit cell, V_{cell} is the unit cell volume, E_{att} is the attachment energy, d_{hkl} is the d spacing and N_A is Avogadro's number.

The area of these faces was compared to scanning electron micrographs of two extreme ibuprofen habits and altered in Mercury (CCDC 3.9, 2016) to represent an average particle habit. The fractional area of each face was expressed using Mercury then the particle surface energy was calculated by summing the face contribution to total surface energy based on area.

2.2 Recrystallisation of ibuprofen

(RS)-ibuprofen (40 µm grade, ≥99.8%) was supplied by Pfizer Ltd and was recrystallised from hexane (95%), toluene (>99.5%), acetonitrile (99.8%) and ethanol (>99.5%) purchased from Fisher Scientific (Loughborough, UK). Supersaturated solutions were prepared at the following concentrations: hexane 1.1 g/mL, toluene 1.5 g/mL, acetonitrile 1.3 g/mL and ethanol 1.5 g/mL. The solubility of ibuprofen in various solvents is documented in the following paper and was used a guide for these experiments [28]. These solutions were heated to 60˚C in a jacketed Optimax reactor (Mettler Toledo, Leicester, UK). The stirred solutions were cooled linearly at a rate of 1˚C/min. The solutions were seeded with 1% of starting material prior to nucleation and then further cooled linearly to 0˚C at a rate of 1˚C/min. Product was obtained through filtering through general-purpose laboratory filter paper (Whatman, UK) and dried in an oven at 50˚C for 24 hours. The resultant batches were named according to their crystallisation solvent (i.e. IbuEth is ibuprofen crystallised from ethanol).

2.3 Size and shape characterisation

The recrystallised batches were sieved through a stainless steel sieve (Endecotts Ltd., London, UK) with a mesh size of 150 µm prior to characterisation.

Scanning electron microscopy (SEM) was used to qualitatively assess particle morphology. Electron micrographs were captured using a Zeiss SUPRA 40VP (Carl Zeiss Microscopy GmbH, Cambridge, UK). The samples were mounted onto an aluminium pin stub containing sticky carbon tabs and sputter coated with platinum. A voltage of 3.0 kV and working distance of 10 mm were used.

The particle size and shape of the samples were measured with a dynamic image analysis system QICPIC (Sympatec Ltd., Clausthal-Zellerfeld, Germany). A vibratory feeder system (VIBRI, Sympatec) was combined with a dry air disperser (RODOS, Sympatec) and was operated at 0.5 bar pressure. The system operates using a pulsed light source with sub-nanosecond illumination, and the particles were imaged by a high speed camera with a frame rate of 400 frames per second. Single measurements were made using the M6 lens (measuring range of 5 – 1705 µm) and a minimum of 200,000 particles were imaged for each run. Images were analysed using WINDOX (Sympatec) software with the size and shape distributions reported using the maximum Feret diameter in order to not lose valuable shape information.

2.4 Physico-chemical characterisation

Powder X-ray diffraction (PXRD) was performed by preparing the samples using a flat plate diffraction patterns collected on a D4 Endeavor (Bruker Corporation, Billerica, Massachusetts, USA). The scan was carried out between 2° and 55° 2θ using CuKα radiation with a secondary graphite monochromator.

Differential scanning calorimetry (DSC) was performed in dry nitrogen gas using a Discovery DSC (TA Instruments – A division of Waters Ltd, Herts, UK). The DSC was calibrated using indium at heating rate of 10°C/min. The samples (2.5 – 3 mg) were analysed in a T-zero standard pan at heating rate of 10°C/min over the range from 30°C to 100°C. Due to sample limitations only one measurement was made.

Headspace gas chromatography (HS-GC) was performed using a 6892N Network GC system coupled to a 7694 HS sampler (Agilent Technologies, CA, US). Around 20 mg of each sample was dissolved in N,N-dimethylacetamide (≥99%) purchased from Sigma Aldrich (Dorset, UK). A liquid-vapour equilibrium was established by heating the solution in a sealed vial and an aliquot of the headspace vapour was analysed by capillary GC. Quantification of each volatile impurity was achieved by comparison of the chromatographic peak areas of external reference standards with the peak areas of the test sample solutions.

2.5 Sticking propensity

The sticking propensity was measured using a Gamlen Tablet Press (GTP-1, Gamlen Tableting Limited, Nottingham, UK). 100 mg of sample was compacted in a 6 mm die at the following pressures: 40 MPa, 120 MPa and 180 MPa at a speed of 60 mm/min. A novel approach to quantify the amount of powder adhered to the base die was developed and is illustrated in Figure 1. Prior to tablet ejection, the detachment stress of the base die was measured manually using a 50 kg hand held force gauge (Mecmesin, Slinfold, UK) placed at the side of the base die. Detachment measurements were made in triplicate.

2.6 Surface Analysis

The specific surface area, pore size distributions and pore volume of the samples was measured using a TriStar II 3020 (Micromeritics U.K. Ltd., Hexton, UK). Between 450 – 850 mg of sample was filled into 3/8'' flat bottom cell with filler rods and conditioned under a helium purge at 40 °C for 16 hours. Nitrogen isotherms were measured at -196 °C. The BET model [29] based on the linear region of the nitrogen adsorption isotherm (from p/p°=0.05 - 0.9) was used for data calculation. Each batch was measured in duplicate.

Surface energy heterogeneity was measured using inverse gas chromatography - surface energy analyser 2.0 (iGC-SEA, Surface Measurement Systems (SMS) Ltd., Alperton, UK). The samples were packed into 4 mm pre-silanised glass columns and mechanically tapped for 10 minutes using SMS sample packing device. All samples were packed to yield a total surface area of approximately 0.13 m^2. The columns were pre-conditioned at 30 °C and 0% RH using helium (carrier gas) at a flow rate of 7 standard cubic centimetres per minute for 120 minutes and these conditions were maintained throughout the experiment duration. A range of dispersive (non-polar) probes (decane, nonane, octane, heptane and hexane) and specific (polar) probes (ethyl acetate and chloroform) were injected at a range of surface coverages (n/n_m) ranging from 1 to 20%; the column dead volume was determined using methane. Data analysis was performed using the Cirrus Plus SEA Data Analysis software (v1.2, SMS Ltd., Alperton, UK). The Dorris/Gray approach [30] was used to determine the dispersive energy contribution, whereas the specific energy contribution was determined by measuring the free energy desorption of a pair of mono-functional acidic and basic probes (chloroform and ethyl acetate), based on the polarisation approach [31] and Della Volpe scale [32]. Detailed reviews of these approaches can be found elsewhere [33, 34]. The repeatability and reproducibility of the iGC-SEA system is quoted by the manufacturer as RSD = 1% [35] which is lower than traditional

iGC techniques due to the system using the same pipe line and injection manifold for every injection [36]. To assess the instrument repeatability batch IbuEth was run in triplicate, but all other batches were run once due to limitations in availability of the iGC-SEA system.

3 Results and Discussion

3.1 Crystal Chemistry

The molecular structure of ibuprofen consists of a phenyl ring with a propanoic acid group and isobutyl in the para position. The structure can be further divided into four molecular components: A) isobutyl, B) phenyl, C) methyl attached to carbon backbone and D) carboxylic acid. The unit cell, for the crystal structure of ibuprofen (IBPRAC), compromises of four molecules arranged in centro-symmetric hydrogen bonded dimers with dimensions a = 14.667 Å, b = 7.886 Å, c = 10.730 Å and ß = 99.362° (Figure). The hydrogen bonding distance is 1.624 Å. This distance is slightly shorter than the mean value of the hits (1601) returned for carboxylic acid hydrogen bonding search in the Cambridge Structural Database (**CSD)**, 1.743 Å, which suggests that this interaction will be strong.

3.1.1 Lattice Energy and Intrinsic Synthons

The calculated lattice energy was -125.2 kJ/mol which is in excellent agreement with experimental sublimation enthalpies of 125.9 kJ/mol [26] and 115.9 kJ/mol [37].

The different intrinsic synthon types were investigated and the six key interactions (>4 kJ/mol) are shown in Figure 3 A total of nine interactions compromising of six types make up 82% of the lattice energy, with the largest contribution coming from the carboxylic acid dimer with a value of -33.7 kJ/mol. This was compared to Dunitz and Gavezzotti's [18] value of -35 kJ/mol for these types of interactions which validates that the forcefield used has accurately predicted the strength of the interaction energy for this short hydrogen bonded dimer.

The strength of this interaction is highlighted by comparing its contribution to lattice energy with the next strongest π-π stacking interaction which contributes 9% compared with 27%, a three-fold difference. The five other interaction types are Van der Waals interactions and despite being crucial for the formation of the crystal are all relatively weak in comparison to the carboxylic acid dimers.

The lattice energy was collapsed onto the individual atoms and summed across each molecular component and reveals that the strongest intermolecular synthon in the crystal structure is the H bonded carboxylic acid (molecular component D), with its contribution to the lattice energy of 37.5%. The molecular components can also be ranked in terms of their increasing contribution to the lattice energy: D>A>B>C Figure 4.

3.1.2 Ibuprofen Morphology Prediction

The Bravais, Friedel, Donnay and Harker (BFDH) morphology of ibuprofen is shown in Figure a and reveals six predicted morphologically important faces. The attachment energy morphology is shown in Figure b and reveals a flatter habit with the disappearance of faces {1 0 -2}, {0 1 1} and the appearance of {1 1 1}. Although this morphology is similar to what is observed experimentally, literature reveals that the three dominant faces during crystallisation are {1 0 0}, {0 0 2} and {0 1 1} [25-27]. The first two faces are present in both the BDFH and attachment energy models however

face {0 1 1} is only present in the BDFH prediction. The attachment energy model was altered to include the three faces present during crystallisation and this is shown in Figure c.

3.1.3 Surface chemistry of ibuprofen

Analysis of the three main faces reveals different crystal chemistry present at the surface of each, as shown in Figure 6 . The dominant (1 0 0) face contains the aliphatic chains; group A at the surface with the molecules linked by the carboxylic acid dimers in the centre of the bulk. This high energy interaction accounts for the directional growth of ibuprofen crystals in the [1 0 0] direction and is confirmed by the lath shaped particles usually produced during crystallisation from non-polar solvents, such as hexane [26]. The (0 1 1) and (0 0 2) face have the carboxylic acid group exposed at the surface allowing for potential hydrogen bonding to occur with Lewis bases. This is confirmed by the habit change when polar crystallisation solvents, such as ethanol, are used and result in a plate like habit due to the slower growth of the (0 1 1) and (0 0 2) face [25, 26].

It is evident from the different chemical functionalities present at each surface that the faces will exhibit different surface energies. In order to view this qualitatively, colour coded images relating to the intrinsic synthon contribution to lattice energy for each surface are shown in Figure 7.

Analysis of the dominant (1 0 0) face reveals that the extrinsic synthon exposed at this face is A. This group is the aliphatic chain and both top and side views of this face show that the surface is flat with no exposure of the other synthons suggesting a relatively low surface energy. Moving to face (0 0 2) the side view reveals that the molecules run at an angle in relation to the surface exposing extrinsic synthons C and D. Synthon C is the lowest energy group however synthon D is the carboxylic acid group involved in the dimer meaning this has to be broken for exposure of this extrinsic synthon. The top view of this face reveals that synthon D is slightly covered by synthon C but is still exposed at the surface. On inspection of the side view of the (0 1 1) face it can be seen that the molecules run parallel to the surface exposing synthon A, C and D. The top view of this face shows that the highest energy synthon (D) is fully exposed and forms channels which imply that this face has high energy due to the dimer not being fully saturated. Qualitative analysis of the three faces ranks them in the following order of increasing surface energy (0 1 1) > (0 0 2) > (1 0 0).

The surface energies of these faces were calculated and these predict the same trends from the qualitative analysis. Face (1 0 0) exhibits the lowest surface energy of 30.7 mJ/m^2. Face (0 0 2) exhibits a higher surface energy of 47.1 mJ/m^2 due to the slight exposure of Group D and the full exposure of this group increases the surface energy of face (0 1 1) to 73.8 mJ/m^2.

The particle surface energies of the two extreme habits of ibuprofen can be compared, where it can be seen that particles crystallised from polar solvents (e.g. ethanol) which contain a more regular habit exhibit a higher particle surface energy ~48.4 mJ/m^2 than the surface energy of needle-like habit crystallised from non-polar solvents (e.g. hexane) ~38.8 mJ/m^2. These predictions are in agreement with the expected results that an increase in solvent polarity increases the fractional surface coverage of the higher energy faces and in turn results in a larger particle surface energy.

3.2 Size and shape characterisation of recrystallised batches

Scanning electron micrographs for recrystallised batches are shown in Figure where differences in particle habit are observed. As expected, increasing the solvent polarity

(hexane<toluene<acetonitrile<ethanol) increases the shape regularity such that the particles change from needle/lath shaped particles to plate/prismatic shaped.

Particle size and shape analysis (QICPIC) was performed on all batches and the number weighted distributions (most sensitive to smaller particles in the sample) are shown in Figure a and the volume weighted distributions (most sensitive to the large particles in the sample) are shown in Figure b. It should be noted that although the batches were passed through a 150 µm sieve they all contain a proportion of particles greater than this. This is due to elongated particles passing through the mesh along their shortest axis and also reporting the data using Feret Max. IbuAce contains the highest proportion of fine (~5 µm) particles and the lowest proportion of coarse material (50 – 400 µm). The volume distribution for this batch is observed to be centered ~250 microns which is higher than all other batches (centered at ~125 µm), inferring that this batch has the widest size distribution. All other batches contain a similar proportion of particles by number and have primary modes centering around 125 µm by volume.

The aspect ratio (width/length) versus particle size (40 - 400 µm) of the batches is shown in **Error! Reference source not found.** and ranks the batches as follows in terms of decreasing aspect ratio ethanol > acetonitrile > toluene > hexane. This data confirms the visual observation that increasing solvent polarity in turn increases shape regularity.

3.3 Physico-chemical characterisation

It was expected that no form change, from *(RS)*-ibuprofen form I, would occur during the recrystallisation of ibuprofen as the only other form reported, form II [38], was prepared by annealing. PXRD was performed to confirm this result. The diffraction patterns for the recrystallised batches are shown in Figure and reveal that all peaks are aligned. Perhaps not unexpectedly, there is some impact on the PXRD intensities due to the texture of the samples. Some preferred orientation is seen in Figure 10 especially from needles crystallised from hexane (a). From the single crystal data it is known where every major peak for form I should be and all the PXRD patterns in Figure 10 are consistent with that. The DSC data (Figure 11) also shows all four samples are form I. This data confirms that no form change has occurred during the recrystallisation and that the form present is *(RS)*-ibuprofen form I due to the mild crystallisation conditions.

The DSC thermograms for all samples are shown in Figure and reveal no major differences between the melt of the samples. The onset of the melt was extrapolated using Trios software (TA Instruments – A division of Waters Ltd, Herts, UK) and was shown to be similar for all samples, with the range 73.7 - 74.5˚C. The peak melting temperatures were found to be within the range 75.8 – 76.1˚C, again confirming that no form changes had occurred during recrystallisation and all samples are of similar crystallinity. The enthalpy of fusion values for recrystallised ibuprofen batches were shown to be; 123.2 J/g for hexane, 126.8 J/g for toluene, 127.4 J/g for acetonitrile and 118.6 J/g for ethanol. It can be seen that there is some variation between the samples, however they are all form I as the reported enthalpy of fusion for form II is 33.9 J/g and unstable at room temperature [38].

The respective volatile organic solvent for each recrystallised batch were quantified using HS-GC and the resultant residual solvent levels are shown to be low (≤180 PPM) and are below the maximum acceptable daily exposure guidelines, as set be ICH Q3C (R6) 2016.

3.4 Sticking Propensity

The sticking propensity of the batches was measured by recording the detachment stress from the base die post compaction. It is proposed that higher stresses relate to more powder adhering to the die in turn inferring a greater sticking propensity. The detachment stress measurements at 3 compaction pressures are shown in Table 1. At the lowest compaction pressures all samples exhibit no sticking and low detachment stress readings (≤0.1 MPa). As the pressure increases the detachment stress values diverge and the largest difference is observed at the highest compaction pressure (~180 MPa) where batches can be ranked as follows in terms of sticking propensity: IbuHex<IbuTol<IbuAce<IbuEth. When sticking is observed the standard deviations of the measurements generally increase and large variation is observed at 108 MPa for IbuEth however the sticking trend is still clear. From this it can be concluded that the sticking propensity of the batches can be ranked in terms of particle habit with an increase in aspect ratio resulting in an increase in sticking propensity

3.5 Surface Analysis

The BET surface area values are presented in Table 2 and show that despite the change in crystal habit the surface area of the particles remains similar, with values between 0.082 - 0.109 m^2/g. The cumulative pore area and volume are also shown in Table 2, where no correlation with sticking propensity can be observed.

Typical isotherms for all batches, as shown in Figure 12, classify all batches as *Type II: non-porous or macroporous* according to the IUPAC guidelines [39]. These results suggest that surface area and pore size are not contributing factors to the observed differences in the sticking propensity of the different habits.

Surface energy heterogenity was calculated for all batches and split into total and dispersive/specific contributions. Studies have suggested surface energy values close to 'infinite dilution' should be reported due to the high energy sites being analysed and hence these values being representative of the entire material surface properties [36]. In order to achieve this, energy values are typically reported at surface coverages of <5%.

The total surface energy (γt) is shown in Table 3 and reveals that the batches IbuAce, IbuTol and IbuHex would rank differently depending on what surface coverage value below 5% was reported. Despite this it is clear that batch IbuEth exhibits the highest total surface energy at all analysed surface coverages (at 1% surface coverage IbuEth has a total surface energy of 67.3 mJ/m^2 whereas all other batches exhibit lower values between 61.1 – 62.0 mJ/m^2).

The same trends are seen from the specific surface energy (γab) values, Table 3, where IbuEth exhibits a higher specific component at all surface coverages compared to all other batches (at 1% surface coverage batch IbuEth has a specific surface energy of 26.4 mJ/m^2 whereas all other batches exhibit lower values between 20.7 – 20.8 mJ/m^2). These results agree with the computational work described where crystallisation in a polar solvent (e.g. ethanol) results in particles with a higher aspect ratio due to the greater exposure of the (0 0 2) and (0 1 1) faces. These faces contain a higher surface energy due to the presence of the carboxylic acid groups at the surface and in turn increase the specific surface energy.

At surface coverages below 5% the dispersive surface energy for all batches was similar, with values between 40.3 – 41.8 .7 mJ/m^2. The dispersive surface energy was unable to be ranked and reveals

that the changes in the total surface energy are due to to the variations in specific surface energy only. This implys that the proportion of the main (1 0 0) face stays constant during particle growth and only the proportion of the (0 0 2) and (0 1 1) face are altered when the polarity of the crystallisation solvent is increased.

It would be expected that the total surface surface energy (influenced by the specific surface energy) would decrease as the aspect ratio of particles decreases. These trends are not observed for IbuAce, IbuHex and IbuTol and these batches would be ranked the same if error is accounted for. This could be due to instrument sensitiviy however an increase in specific surface energy as aspect ratio increases can be inferred from the computational work. Batch IbuEth contains the highest specific surface energy and exhibits the highest sticking propensity. If the findings from the computational work are taken into acount then sticking propensity increases as specific surface energy increases. Previous work has shown that a higher surface energy leads to greater cohesion therefore a higher tensile strength of tablets [40]. The findings from this study suggest that the specific contribution to the total surface energy may alter the adhesive properties and a higher specific component leads to greater adhesion and therefore sticking propensity.

It should be noted here that the computational data is derived from a bottom-up approach where the energy is calculated from the unsaturated interactions at the surface of the face. The iGC data is based on a top-down approach where the energy is derived from interactions at the surface from the highest energy sites. In order to compare the two techniques caution must be taken when reporting iGC data due to different surface coverages. It is proposed that as computational modelling accounts for the whole surface and not just high energy sites then reporting iGC at infinite dilution would not be suitable for this comparison. The total surface energy (at 20% surface coverage) for needles is 56.0 mJ/m2 compared to 65.1 mJ/2 for prisms. This is a 9.1 mJ/m2 increase for the prisms compared to the needles and the calculated surface energy reveals a similar increase of 9.6 mJ/2 (needles: 38.8 mJ/m2 and prisms: 48.4 mJ/m2). These values are not alingned due to the differences in the approaches descirved above however do show excellent agreement in the differences.

4 Conclusion

The crystal chemistry of ibuprofen was explored and the importance of the hydrogen bonded carboxylic acid dimers contribution to lattice energy was revealed. The surface chemistry of the three dominant faces was visualised in relation to lattice energy and the calculated surface energy values of the faces increased as the exposure of the carboxylic acid group increased.

The different surface chemistries enabled the proportion of each face to be altered by crystallisation in solvents with differing polarity and ibuprofen was successfully crystallised into four diverse particle habits. The sticking propensity of these batches was shown to be driven by the changes in particle habit, where a more regular particle habit resulted in the material demonstrating a higher degree of sticking. To further investigate if the sticking propensity was driven by a chemical change altered by the difference in physical shape the surface energy of particles was explored.

The particle surface energies of the extreme habits were compared experimentally by iGC and computationally. Although the absolute values did not align both approaches showed that prism shaped particles exhibited a higher energy of around 9 mJ/m^2 compared to needles. The iGC and qualitative modelling data further revealed this difference to be attributed to the increase in the specific (polar) component, which is due to greater presence of faces which contain the carboxylic acid functionality at the surface.

The combination of experimental and computational surface energy techniques reveal that the sticking propensity of ibuprofen is increased by a change in specific surface energy caused by a change in crystal habit. Computational and experimental data reveals that the increase in surface energy of the regular shaped particles can be attributed to the increase in the specific (polar) component, which is due to greater presence of faces which contain the carboxylic acid functionality at the surface. The increase in the specific energy component is shown to correlate with the sticking propensity of ibuprofen. It is proposed that investigation of the chemical causality of sticking, for this API and others, using the techniques demonstrated in this paper will be of increasing importance.

5 Funding Sources

This work was supported by Global Technology Services, Pfizer Global Supply

6 Acknowledgements

Ivan Marziano and Adrian Daly are thanked for their guidance and expertise regarding the recrystallisation work.

References

1. Challener, C.A., *QbD in API Manufacture: With a quality-by-design approach, robust processes consistently can help deliver quality product.* Pharmaceutical Technology, 2014. **38**(9).
2. Shekunov, B.Y., P. Chattopadhyay, H.H.Y. Tong, and A.H.L. Chow, *Particle Size Analysis in Pharmaceutics: Principles, Methods and Applications.* Pharmaceutical Research, 2007. **24**(2): p. 203-227.
3. Chow, K., H.H.Y. Tong, S. Lum, and A.H.L. Chow, *Engineering of pharmaceutical materials: An industrial perspective.* Journal of Pharmaceutical Sciences, 2008. **97**(8): p. 2855-2877.
4. Sun, C.C., *Materials science tetrahedron—A useful tool for pharmaceutical research and development.* Journal of Pharmaceutical Sciences, 2009. **98**(5): p. 1671-1687.
5. Storey, R.A., R. Docherty, and P.D. Higginson, *Integration of high throughput screening methodologies and manual processes for solid form selection.* Am. Pharm. Rev., 2003. **6**: p. 104-105.
6. Ticehurst, M. and R. Docherty, *From molecules to pharmaceutical products – the drug substance/drug product interface.* Am. Pharm. Rev., 2006. **9**: p. 34-36.
7. Waknis, V., E. Chu, R. Schlam, A. Sidorenko, S. Badawy, S. Yin, and A. Narang, *Molecular Basis of Crystal Morphology-Dependent Adhesion Behavior of Mefenamic Acid During Tableting.* Pharmaceutical Research, 2014. **31**(1): p. 160-172.
8. Paul, S., K. Wang, L.J. Taylor, B. Murphy, J. Krzyzaniak, N. Dawson, M.P. Mullarney, P. Meenan, and C.C. Sun, *Dependence of Punch Sticking on Compaction Pressure—Roles of Particle Deformability and Tablet Tensile Strength.* Journal of Pharmaceutical Sciences, 2017. **106**(8): p. 2060-2067.
9. Paul, S., L.J. Taylor, B. Murphy, J. Krzyzaniak, N. Dawson, M.P. Mullarney, P. Meenan, and C.C. Sun, *Mechanism and Kinetics of Punch Sticking of Pharmaceuticals.* Journal of Pharmaceutical Sciences, 2017. **106**: p. 151-158.
10. Roberts, M., J.L. Ford, G.S. MacLeod, J.T. Fell, G.W. Smith, P.H. Rowe, and A.M. Dyas, *Effect of punch tip geometry and embossment on the punch tip adherence of a model ibuprofen formulation.* Journal of Pharmacy and Pharmacology, 2004. **56**(7): p. 947-950.
11. Danjo, K., S. Kojima, C.Y. Chen, H. Sunada, and A. Otsuka, *Effect of Water Content on Sticking during Compression.* CHEMICAL & PHARMACEUTICAL BULLETIN, 1997. **45**(4): p. 706-709.

12. Roberts, M., J.L. Ford, P.H. Rowe, A.M. Dyas, G.S. MacLeod, J.T. Fell, and G.W. Smith, *Effect of lubricant type and concentration on the punch tip adherence of model ibuprofen formulations.* Journal of Pharmacy and Pharmacology, 2004. **56**(3): p. 299-305.
13. Pudasaini, N., P.P. Upadhyay, C.R. Parker, S.U. Hagen, A.D. Bond, and J. Rantanen, *Downstream Processability of Crystal Habit-Modified Active Pharmaceutical Ingredient.* Organic Process Research & Development, 2017.
14. Sun, H., *COMPASS: An ab Initio Force-Field Optimized for Condensed-Phase Applications Overview with Details on Alkane and Benzene Compounds.* The Journal of Physical Chemistry B, 1998. **102**(38): p. 7338-7364.
15. Clark, M., R.D. Crammer III, and N.V. Opdenbosch, *Validation of the General Purpose Tripos 5.2 Force Field.* Journal of Computational Chemistry, 1989. **10**: p. 982-1012.
16. Clydesdale, G., R. Docherty, and K.J. Roberts, *HABIT - a program for predicting the morphology of molecular crystals.* Computer Physics Communications, 1991. **64**(2): p. 311-328.
17. Clydesdale, G., K.J. Roberts, and R. Docherty, *HABIT95 — a program for predicting the morphology of molecular crystals as a function of the growth environment.* Journal of Crystal Growth, 1996. **166**(1–4): p. 78-83.
18. Dunitz, J.D. and A. Gavezzotti, *Supramolecular Synthons: Validation and Ranking of Intermolecular Interaction Energies.* Crystal Growth & Design, 2012. **12**(12): p. 5873-5877.
19. Bravais, A., *Etudes Crystallographiques*. 1866, Paris: Gauthiers Villars.
20. Friedel, G., *Bulletin De La Societe Francaise De Mineralogie Et De Crystallographie.* 1907. **30**: p. 326.
21. Donnay, J.D.H. and D. Harker, *A new law of crystal morphology extending the law of bravais.* Am Mineral, 1937. **22**: p. 446-467.
22. Docherty, R., G. Clydesdale, K.J. Roberts, and P. Bennema, *Application of Bravais-Friedel-Donnay-Harker, attachment energy and Ising models to predicting and understanding the morphology of molecular crystals.* Journal of Physics D: Applied Physics, 1991. **24**(2): p. 89.
23. Rosbottom, I., K.J. Roberts, and R. Docherty, *The solid state, surface and morphological properties of p-aminobenzoic acid in terms of the strength and directionality of its intermolecular synthons.* CrystEngComm, 2015. **17**(30): p. 5768-5788.
24. Hartman, P. and P. Bennema, *The attachment energy as a habit controlling factor.* Journal of Crystal Growth, 1980. **49**(1): p. 145-156.

25. Cano, H., N. Gabas, and J.P. Canselier, *Experimental study on the ibuprofen crystal growth morphology in solution.* J. Cryst. Growth, 2001. **224**: p. 335–341.
26. Bunyan, J., N. Shankland, and D. Sheen, *Solvent Effects on The Morphology of Ibuprofen.* AIChE Symp. Ser., 1991: p. 45-57.
27. Winn, D. and M.F. Doherty, *Modeling crystal shapes of organic materials grown from solution.* AIChE Journal, 2000. **46**(7): p. 1348-1367.
28. Nguyen, T.T.H., R.B. Hammond, K.J. Roberts, I. Marziano, and G. Nichols, *Precision measurement of the growth rate and mechanism of ibuprofen {001} and {011} as a function of crystallization environment.* CrystEngComm, 2014. **16**: p. 4568-4586.
29. Brunauer, S., P.H. Emmett, and E. Teller, *Adsorption of Gases in Multimolecular Layers.* Journal of the American Chemical Society, 1938. **60**(2): p. 309-319.
30. Dorris, G.M. and D.G. Gray, *Adsorption of n-alkanes at zero surface coverage on cellulose paper and wood fibers.* Journal of Colloid and Interface Science, 1980. **77**(2): p. 353-362.
31. Dong, S., M. Brendlé, and J.B. Donnet, *Study of solid surface polarity by inverse gas chromatography at infinite dilution.* Chromatographia, 1989. **28**(9): p. 469-472.
32. Volpe, C.D. and S. Siboni, *Some Reflections on Acid–Base Solid Surface Free Energy Theories.* Journal of Colloid and Interface Science, 1997. **195**(1): p. 121-136.
33. Shi, B., Y. Wang, and L. Jia, *Comparison of Dorris-Gray and Schultz methods for the calculation of surface dispersive free energy by inverse gas chromatography.* Journal of Chromatography A, 2011. **121B**: p. 860-862.
34. Ho, R. and J.Y.Y. Heng, *A Review of Inverse Gas Chromatography and its Development as a Tool to Characterize Anisotropic Surface Properties of Pharmaceutical Solids.* KONA Powder and Particle Journal, 2013. **30**: p. 164-180.
35. SMS. *iGC-SEA compared to Contact Angle (CA) and Atomic Force Microscopy (AFM) - www.surfacemeasurementsystems.com/solutions/inverse-gas-chromatography-sea/*. 2016.
36. Gamble, J.F., M. Leane, D. Olusanmi, M. Tobyn, E. Šupuk, J. Khoo, and M. Naderi, *Surface energy analysis as a tool to probe the surface energy characteristics of micronized materials—A comparison with inverse gas chromatography.* International Journal of Pharmaceutics, 2012. **422**(1–2): p. 238-244.

37. Perlovich, G.L., S.V. Kurkov, L.K. Hansen, and A. Bauer-Brandl, *Thermodynamics of Sublimation, Crystal Lattice Energies, and Crystal Structures of Racemates and Enantiomers: (+)- and (±)-Ibuprofen.* Journal of Pharmaceutical Sciences, 2004. **93**(3): p. 654-666.
38. Dudognon, E., F. Danède, M. Descamps, and N.T. Correia, *Evidence for a New Crystalline Phase of Racemic Ibuprofen.* Pharmaceutical Research, 2008. **25**(12): p. 2853-2858.
39. Sing, K.S.W., D.H. Everett, R.A.W. Haul, L. Moscou, R.A. Pierotti, J. Rouquerol, and T. Siemieniewska, *Reporting physisorption data for gas/solid systems with special reference to the determination of surface area and porosity.* Pure Appl. Chem., 1985. **57**(4): p. 603-619.
40. El Gindy, N.A. and M.W. Samaha, *Tensile strength of some pharmaceutical compacts and their relation to surface free energy.* International Journal of Pharmaceutics, 1982. **13**(1): p. 35-46.

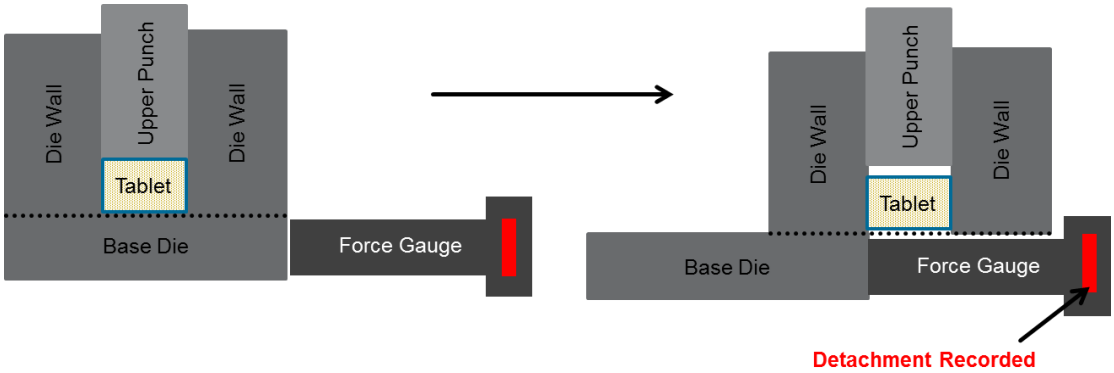

Figure 1 – Gamlen Tablet Press detachment force tool used for the quantification of sticking propensity.

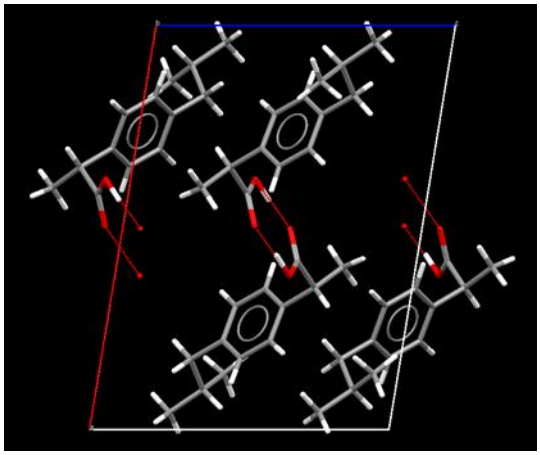

Figure 2 –Ibuprofen unit cell displaying hydrogen bonded carboxylic acid dimers.

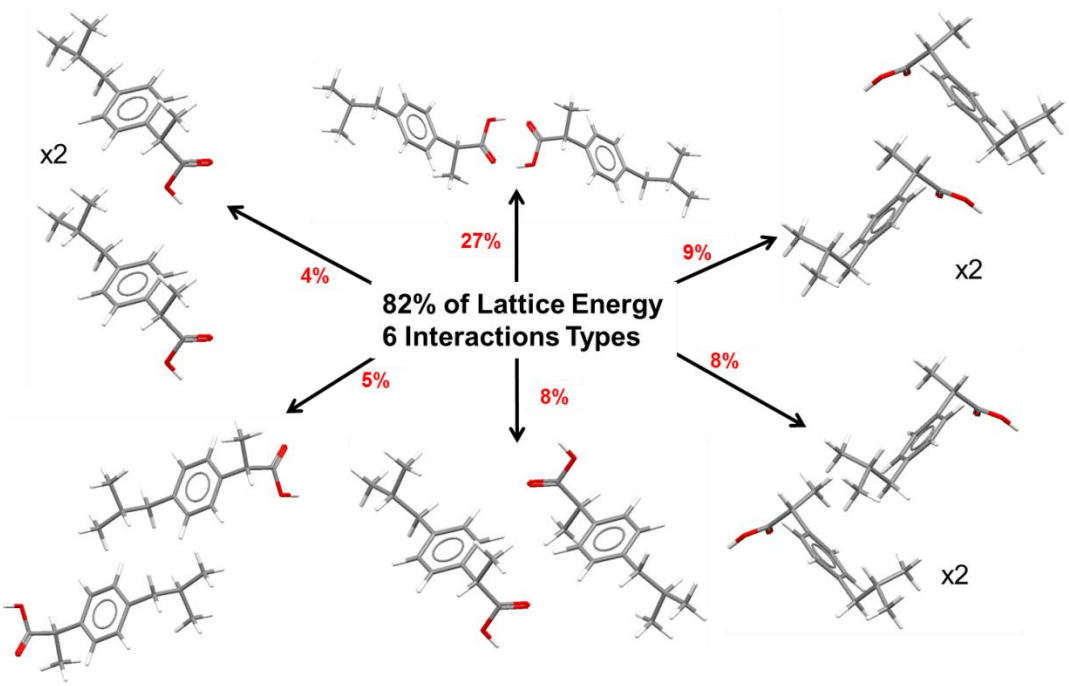

Figure 3 – Key interaction types and their energy contribution to the total lattice energy.

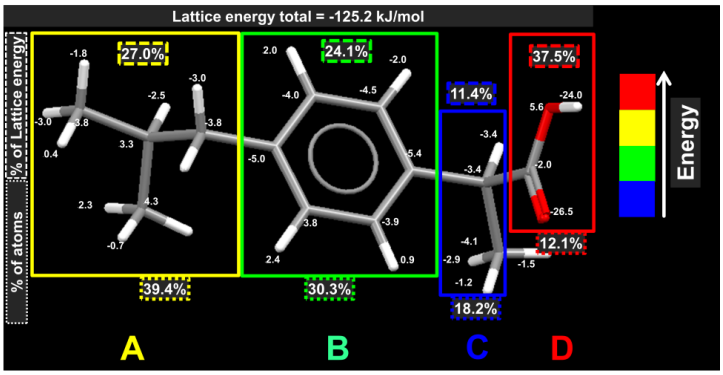

Figure 4 – Energy diagram of the lattice energy contribution from atoms and overall contribution from molecular components.

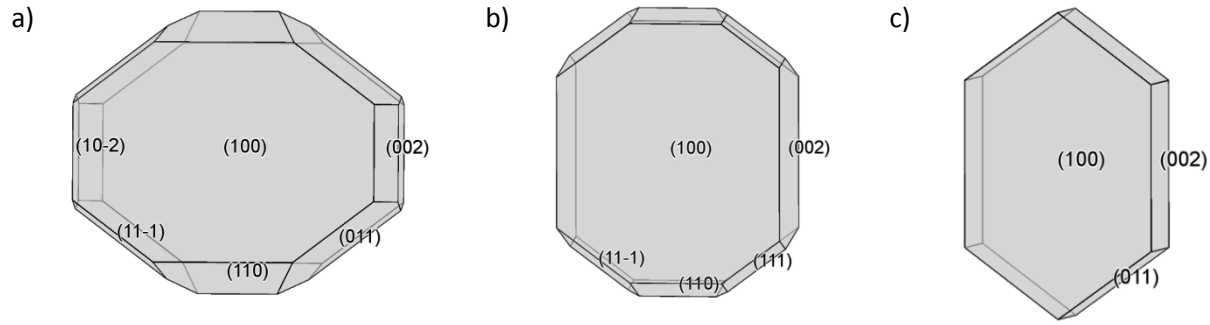

Figure 5 –Predicted morphology of ibuprofen where a) BFDH highlighting six morphologically important crystal faces b) attachment energy morphology highlighting five morphologically important crystal faces c) attachment energy morphology edited to only include the three faces observed during crystallisation.

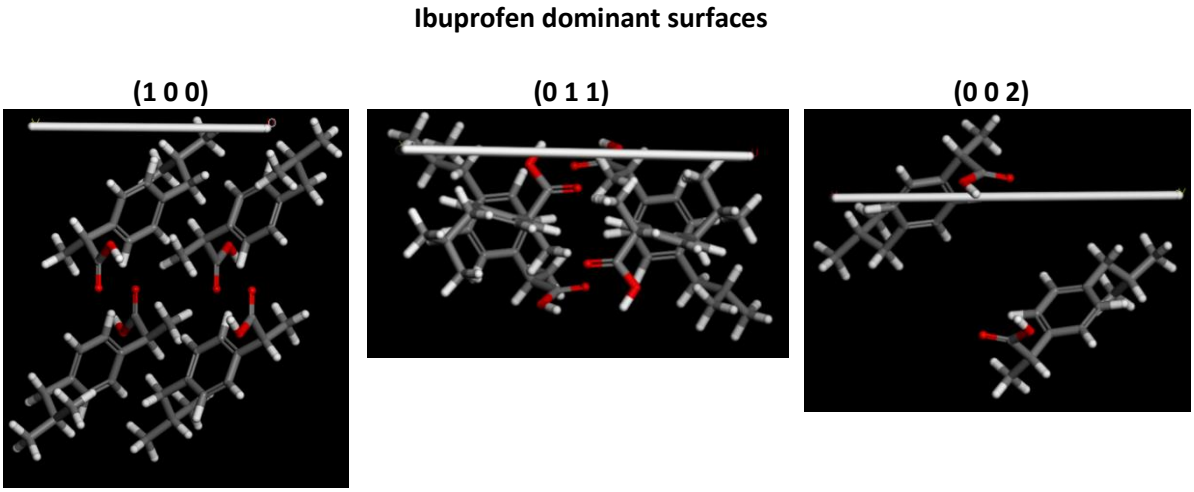

Figure 6 – Crystal chemistry of ibuprofen dominant surfaces.

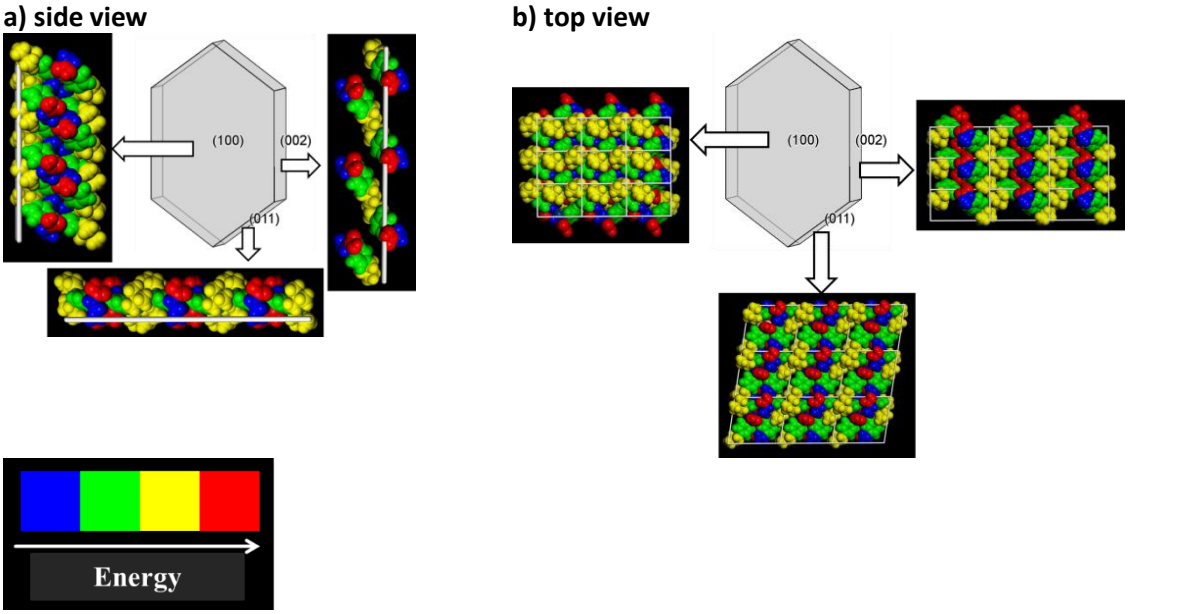

Figure 7 – Crystal chemistry of ibuprofen surfaces colour coded related to the atomic contribution to lattice energy a) side view of the three faces b) top view of the three faces.

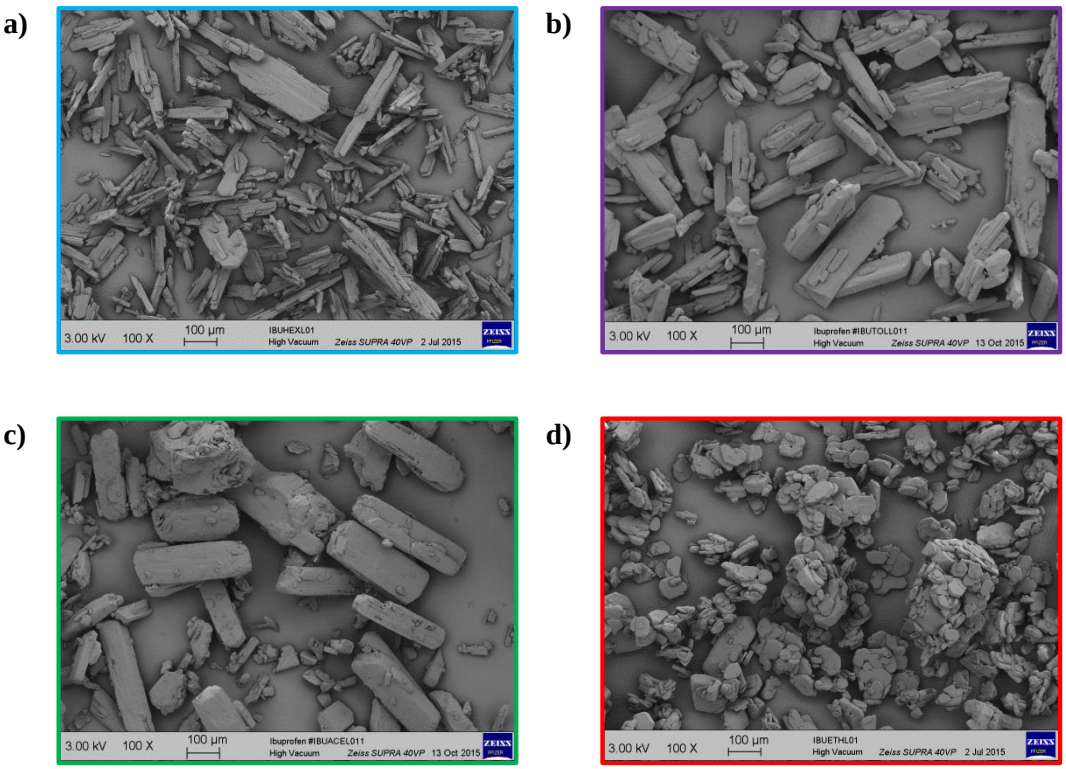

Figure 8 – Scanning electron micrographs of recrystallised ibuprofen showing changes in particle habit from; a) hexane b) toluene c) acetonitrile d) ethanol. All images captured using x100 magnification and scale bar is 100 µm.

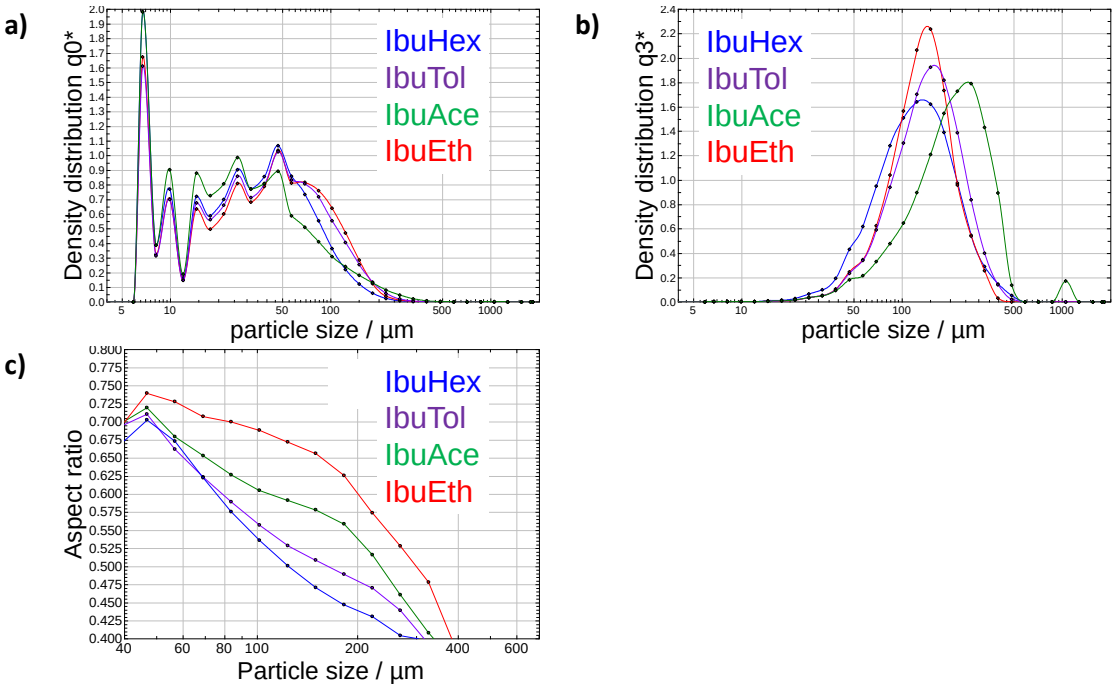

Figure 9 – QICPIC a) number and b) volume weighted distributions for recrystallised ibuprofen batches; c) QICPIC aspect ratio versus particle size for recrystallised batches.

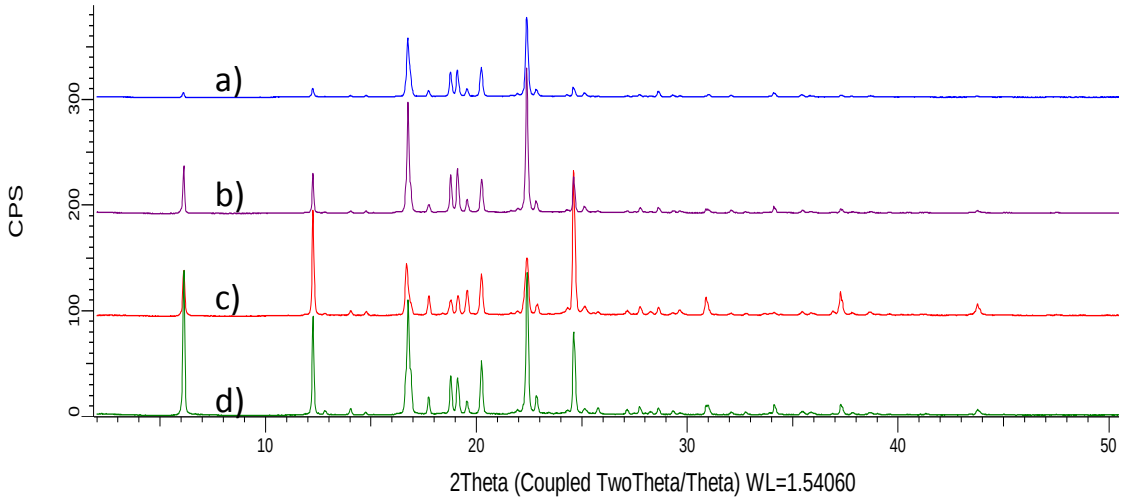

Figure 10 – Powder X-ray diffraction patterns for recrystallised ibuprofen a) hexane b) toluene c) ethanol d) acetonitrile.

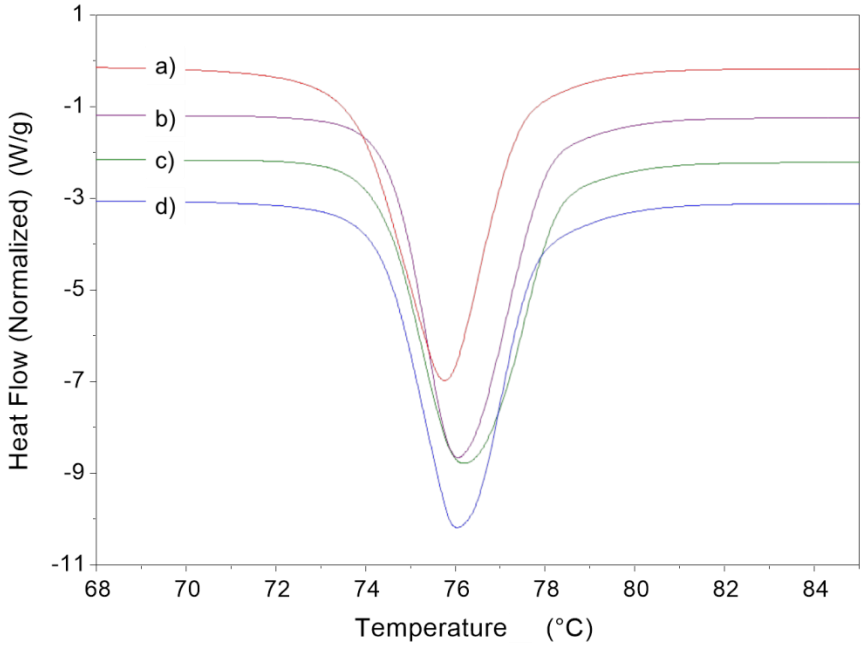

Figure 11 – DSC thermograms of recrystallised ibuprofen a) ethanol b) toluene c) acetonitrile d) hexane.

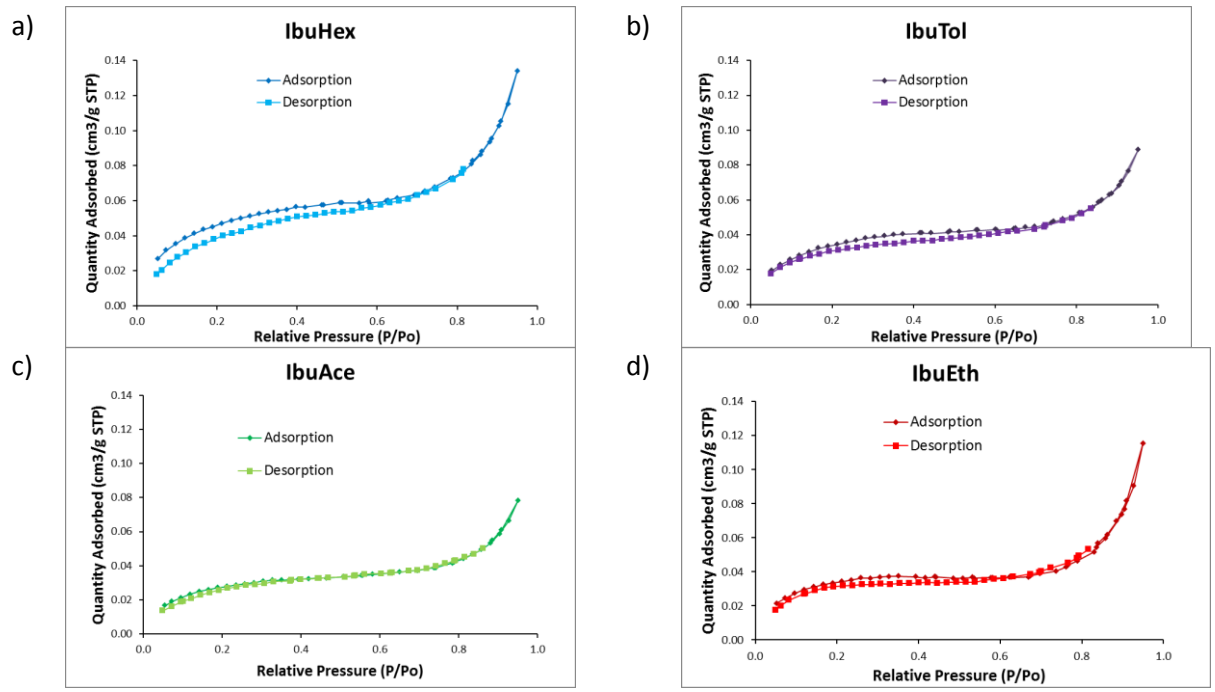

Figure 12 – Typical isotherms for recrystallised ibuprofen batches a) IbuHex b) IbuTol c) IbuAce d) IbuEth

Table 1 – Detachment stress of recrystallised ibuprofen at three compaction pressures. Standard deviation of three measurements are shown in brackets.

	Detachment Stress		
Batch	40 MPa	108 MPa	180 MPa
IbuHex	0.05 (0.01)	0.08 (0.01)	0.50 (0.01)
IbuTol	0.09 (0.02)	0.27 (0.03)	0.72 (0.22)
IbuAce	0.07 (0.01)	0.63 (0.10)	1.97 (0.39)
IbuEth	0.10 (0.01)	3.38 (0.96)	3.37 (0.24)

Table 2 – BET surface area, cumulative pore volume and cumulative pore area for recrystallised ibuprofen samples. Reported values are mean of two measurements.

Batch	BET surface area (m^2/g)	Cumulative pore volume (mm^3/g)	Cumulative pore area (m^2/g)
IbuHex	0.109	0.183	0.114
IbuTol	0.082	0.111	0.070
IbuAce	0.101	0.095	0.054
IbuEth	0.082	0.153	0.074

Table 3 – Surface energy (total γt and specific γab) for recrystallised ibuprofen at different surface coverages. Reported standard deviation shown in brackets is of three measurements made on sample with highest variation in surface energy (IbuEth).

	Surface energy (mJ/m^2)							
	IbuHex		IbuTol		IbuAce		IbuEth	
Surface coverage	γt	γab	γt	γab	γt	γab	γt	γab
1	62.0	20.7	61.9	20.8	61.1	20.7	67.3 (2.4)	26.4 (1.7)
2	60.7	20.1	62.9	21.2	62.1	20.8	67.0 (2.1)	26.2 (1.6)
4	60.9	20.2	59.3	19.0	62.0	20.2	66.6 (1.9)	25.9 (1.5)
6	60.0	19.8	59.1	18.6	57.4	17.7	66.3 (2.0)	25.8 (1.5)
10	57.5	18.8	55.0	16.1	53.5	15.5	65.8 (1.8)	25.5 (1.5)
15	56.4	18.3	56.2	16.7	52.1	14.6	65.4 (1.8)	25.3 (1.5)
20	56.0	18.1	54.9	15.4	50.6	13.8	65.1 (1.5)	25.1 (1.3)